Journal of the Optical Society of Korea
Vol. 20, No. 5, October 2016, pp. 628-632

ISSN: 1226-4776(Print) / ISSN: 2093-6885(Online)
DOI: http://dx.doi.org/10.3807/JOSK.2016.20.5.628

Effective Sensing Volume of Terahertz Metamaterial with Various Gap Widths

Sae June Park, Sae A Na Yoon, and Yeong Hwan Ahn*

Department of Physics and Department of Energy Systems Research, Ajou University, Suwon 16499, Korea

(Received June 28, 2016 : revised September 29, 2016 : accepted September 29, 2016)

We studied experimentally and theoretically the vertical range of the confined electric field in the gap area of metamaterials, which was analyzed for various gap widths using terahertz time-domain spectroscopy. We measured the resonant frequency as a function of the thickness of poly(methyl methacrylate) in the range 0 to 3.2 μm to quantify the effective detection volumes. We found that the effective vertical range of the metamaterial is determined by the size of the gap width. The vertical range was found to decrease as the gap width of the metamaterial decreases, whereas the sensitivity is enhanced as the gap width decreases due to the highly concentrated electric field. Our experimental findings are in good agreement with the finite-difference time-domain simulation results. Finally, a numerical expression was obtained for the vertical range as a function of the gap width. This expression is expected to be very useful for optimizing the sensing efficiency.

Keywords : Terahertz spectroscopy, Metamaterials, Sensor
OCIS codes : (300.6495) Spectroscopy, terahertz; (160.3918) Metamaterials; (280.1415) Biological sensing and sensors

I. INTRODUCTION

In recent years, metamaterials have been intensively studied because they have special properties beyond those of natural materials, such as negative refraction, super lensing, cloaking, perfect absorber, and sensing [1-6]. In the last decade, many types of metamaterial structures were suggested such as single split, double split, and electrical split ring resonators operating across various frequency ranges [7-11]. They consist of an array of metallic resonators that interact with electromagnetic waves. Various resonance modes such as inductive-capacitive (*LC*) resonance, dipole resonance, and quadruple resonance appear in the metamaterials when the circular current is generated by interacting with incident light. The properties of each resonance mode are mainly governed by geometrical factors such as periodicity, gap width, metal thickness, and side arm length [4, 12-15].

The *LC* resonance occurs in metamaterials at a resonant frequency described by $f_0 = 1/(2\pi\sqrt{LC})$, where C is the capacitance of the gap structure and L is the inductance of the side arm structure [4, 14]. Here, the *LC* resonant frequency can be easily controlled by manipulating the parameters C and L. For example, a change in the dielectric constant of the gap area causes a shift in the resonant frequency. Recently, we showed that THz metamaterials can work as sensitive on-site detectors for microorganisms with an extremely low density, both in ambient and aqueous environments [2, 4]. The detection volume of metamaterial sensors is extremely confined in the vicinity of the gap area, providing enhanced sensitivity. More importantly, this enables us to use a very thin water layer, and hence, to overcome the difficulties caused by the strong water attenuation of THz waves [16]. For sensing applications, the effect of the geometrical parameters on the metamaterial resonance, such as the gap width, the metal thickness, and the substrate dielectric constant have been very important properties for device optimization [12-14, 17]. In particular, the vertical extent of the sensing volume has been addressed in slot antenna structures and metamaterials. However, the effective volumes and the sensitivities have not been studied in terms of the gap

*Corresponding author: ahny@ajou.ac.kr
Color versions of one or more of the figures in this paper are available online.

widths of the metamaterials.

In this research, we performed terahertz time-domain spectroscopy (THz-TDS) and finite-difference time-domain (FDTD) simulations to study the effect of gap width on the effective detection volume of the THz metamaterial. We quantified the resonance frequency shift of the THz metamaterials as a function of the polymer thickness and also as a function of the gap width. This enabled us to extract the explicit relation between the vertical range of the detection volume and the gap width.

II. SAMPLE PREPARATION AND EXPERIMENTAL METHODS

We used conventional e-beam lithography, followed by metal deposition of Cr/Au (2 nm/98 nm) to fabricate the THz metamaterials on a quartz substrate with a thickness of 1 mm. The 30×30 THz metamaterials consist of a metamaterial unit cell with a side arm length of 36 μm, a line width of 4 μm, and gap widths of 0.5, 1, 2, and 4 μm, respectively, as shown in Fig. 1(a). A poly(methyl methacrylate) (PMMA) layer was coated repeatedly onto the metamaterial device using a conventional spin coating method and baking processes. The thickness of the PMMA layer (h_{PMMA}) increased by 210 nm each time the spin-coating procedure was repeated.

We used the THz-TDS system to record the transmission of THz waves through the metamaterials. A linearly polarized THz pulse was produced from a photoconductive antenna by illuminating a mode-locked femtosecond laser with λ = 800 nm. The THz beam was focused on the THz metamaterials with an area of ~1 mm^2 under ambient conditions. The amplitude and phase of the transmitted THz field in the time domain were obtained by adjusting the time delay between the THz beam and the probe beam. We obtained the THz spectrum in the frequency domain by calculating the fast Fourier transform (FFT) of the transmitted THz field in the time domain. The THz transmission spectra were recorded with an acquisition time of 5 s for each spectrum.

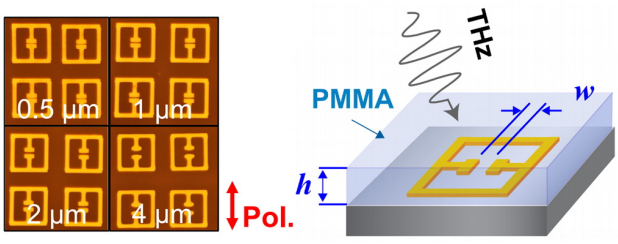

(a) (b)

FIG. 1. (a) Optical microscope images of THz metamaterials with various gap widths (w) of 0.5, 1, 2, 4 μm (b) Experimental schematic for the study of the effective detection volume.

III. RESULTS AND DISCUSSION

Our research involves studying the effective detection volume of THz metamaterial for various gap widths. First, we quantify the effective vertical range as a function of the h_{PMMA} on the THz metamaterial device as shown in Fig. 1(b). The resonant frequency (f_0) changes as the PMMA layer is deposited and its thickness increases.

Figure 2(a) shows the transmission spectra for the PMMA layer with two different thicknesses of 0.21 μm (blue line) and 1.05 μm (red line), for a gap width of 4 μm. The transmission spectra of the uncoated metamaterials are plotted alongside for comparison (black line). The PMMA coating caused the resonant frequency to shift toward the red, which is due to the increased effective dielectric constant in the gap area of the metamaterials [2-4, 11]. As expected, the frequency shift (Δf) is higher for larger h_{PMMA}. As mentioned above, the resonant frequency of the THz metamaterials changes when dielectric materials are coated onto the metamaterial surface because of the change in the dielectric constant in the gap area. The resonant frequency shift can be explained by the following relationship: $\Delta f/f_0 \approx \alpha(\varepsilon_{PMMA} - \varepsilon_{air})/\varepsilon_{eff}$ [2, 4],

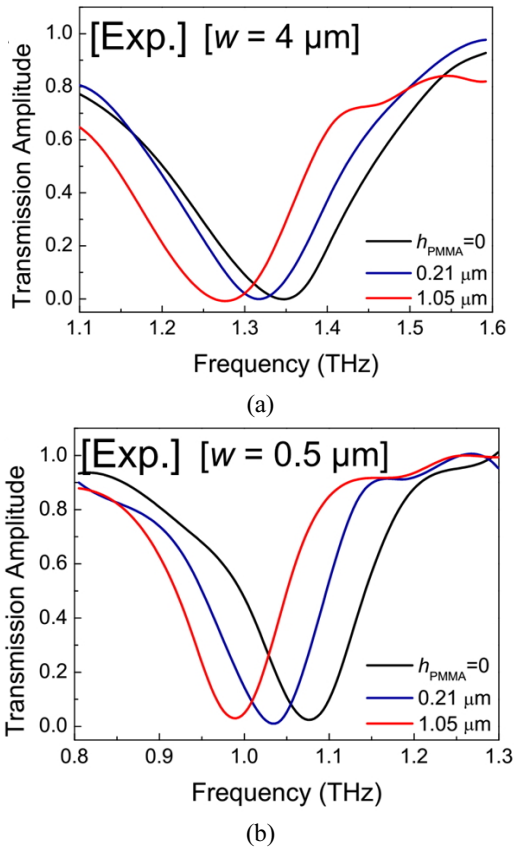

FIG. 2. Transmission spectra for the two different PMMA thicknesses (h_{PMMA}) of 0.21 μm (blue line) and 1.05 μm (red line), and without the PMMA layer (black line) for (a) w = 4.0 μm and (b) w = 0.5 μm.

where α is the sensitivity coefficient, ε_{PMMA} is the dielectric constant of PMMA, ε_{air} is the dielectric constant of air, and ε_{eff} (= n_{eff}^2) is the effective dielectric constant without the PMMA coating. In this work, we determined α to have a value of 0.22, whereas ε_{eff} is known to have a value of 2.96 in the case of quartz [14].

As we are interested in the detection volume and the sensitivity as a function of gap width, we performed the same experiments on the metamaterials with a different width of w = 0.5 μm as shown in Fig. 2(b). It is clear from the spectra that Δf is higher for a smaller gap width of 0.5 μm compared to the large gap width (w = 4 μm) we used previously. This indicates the sensitivity is higher as the gap width decreases. Gap-width dependent sensitivities have been reported for slot antenna structures but have not been reported for metamaterial patterns with positive structures [4, 18]. Furthermore, the detection volume has not been addressed as a function of the gap width.

We studied the effective vertical range of the THz metamaterial for various gap widths by quantifying the value of Δf of the THz metamaterial for the gap widths of 0.5, 1, 2, and 4 μm, as a function of the h_{PMMA}, as shown in Fig. 3(a). The Δf is enhanced as we increase the h_{PMMA} as shown above. In addition, clear saturation behavior was found as the thickness increased. More importantly, we found that saturation thickness (h_{sat}) is reached sooner for samples with smaller gaps. This means that the vertical range of the detection volume can also be expected to be smaller when the gap width is small. By fitting the data with the relation $\Delta f = \Delta f_{sat}(1-\exp(-h_{PMMA}/h_{sat}))$, we plotted h_{sat} as a function of the gap width in Fig. 3(b). We also plotted the sensitivity of the metamaterials sensors with respect to h_{PMMA} as red circles. Here, the sensitivity (S) is defined by the initial slope of the $\Delta f - h_{PMMA}$ curves in Fig. 3(a), leading to $S = \Delta f/h_{PMMA} \approx \Delta f_{sat}/h_{sat}$(for $h_{PMMA} \ll h_{sat}$). The vertical range increases by 2.5 times for w = 0.5 μm relative to that of w = 4.0 μm. Conversely, the sensitivity in terms of the thickness increases from 83.8 GHz/μm (w = 4.0 μm) to 148.4 GHz/μm (w = 0.5 μm), which is an increase of 1.8 times. Considering the fact that f_0 decreases for smaller w, the sensitivity increase in terms of $\Delta f/f_0$ is approximately 2.2.

Our experimental results were confirmed by the Lumerical FDTD simulations [3, 4]. Here, we used a linearly polarized plane wave and a periodic boundary condition to imitate our experiments. We considered the metal film of which the THz metamaterial is composed as a perfect electric conductor. We then mimicked the PMMA layer by using the dielectric constant (ε_{PMMA}=2.56) of PMMA from the literature [19] and varied the h_{PMMA} in the range 0 – 3.2 μm. We first show the 2D field distribution near the gap area along the z-x plane (at y = 0) for both devices with gap widths of 4.0 μm and 0.5 μm in Fig. 4(a) and (b), respectively. The inset in Fig. 4(a) shows the geometry of the pattern near the gap area. As discussed above, the effective detection volume of the THz metamaterial in the gap area is highly confined near the surface and strongly influenced by the gap width. We plotted the electric field amplitude as a function of the vertical position (z) at the center of the gap structure (at $x = y$ = 0) in Fig. 4(c). The vertical range can be roughly estimated from this plot by fitting the exponential function, which yields h_{sat} = 2.5 μm and 0.7 μm, respectively, for w = 4.0 μm and 0.5 μm. Although this simple vertical line plot at the center of the gap (not a full-wave transmission) cannot reproduce our experimental data, these results are in reasonable agreement with our experimental findings shown in Fig. 3.

In Fig. 5(a), the numerically calculated results on Δf (for the full-wave transmission) as a function of the height h of the dielectric materials (with ε = 2.56) are extracted from the transmission spectra for the different gap widths ranging from 0.5 to 4.0 μm. The results are in good agreement with our experimental data in Fig. 3(a). Finally, in Fig. 5(b), we plotted, from the simulation results, the h_{sat} (black boxes)

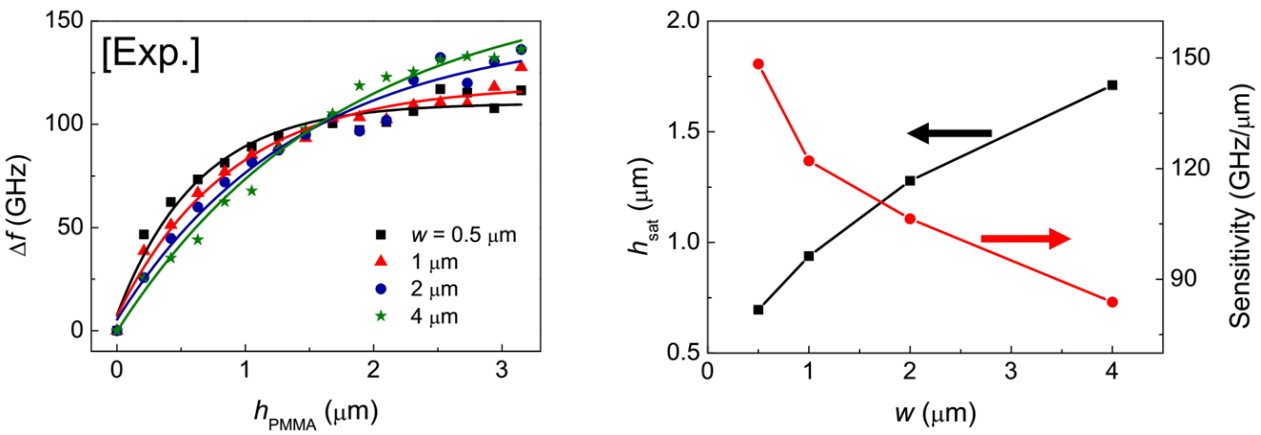

(a) (b)

FIG. 3. (a) Resonant frequency shift (Δf) as a function of h_{PMMA} for various w's in the range of 0.5 – 4.0 μm. (b) Saturation thickness (black boxes) and sensitivity (red circles) as a function of w.

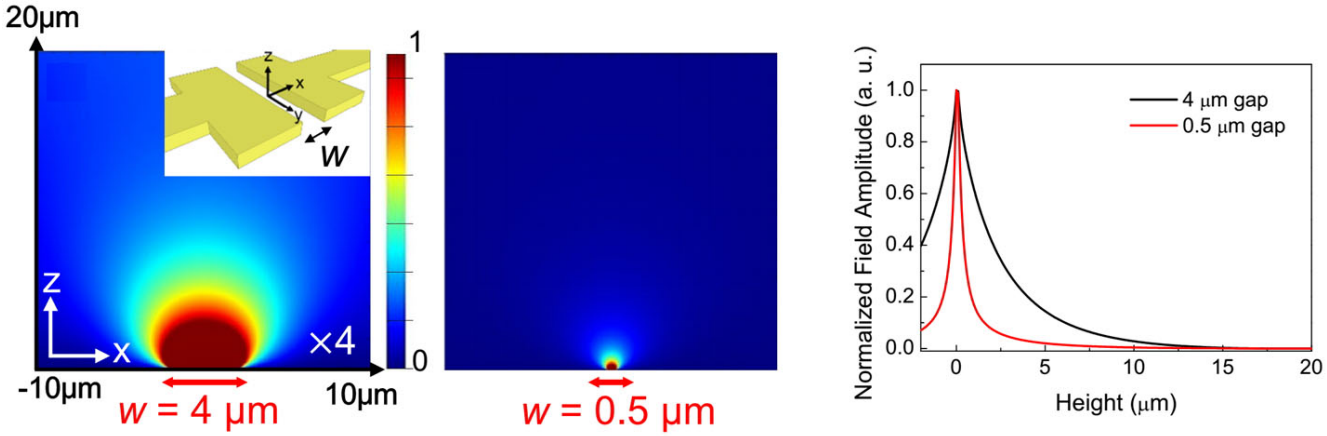

(a) (b) (c)

FIG. 4. Field distribution near the gap area (at $y = 0$) for (a) $w = 4.0$ μm and (b) $w = 0.5$ μm. (c) The electric field line profiles at the center of the gap structure along the z-axis, extracted from (a) (black line) and (b) (red line).

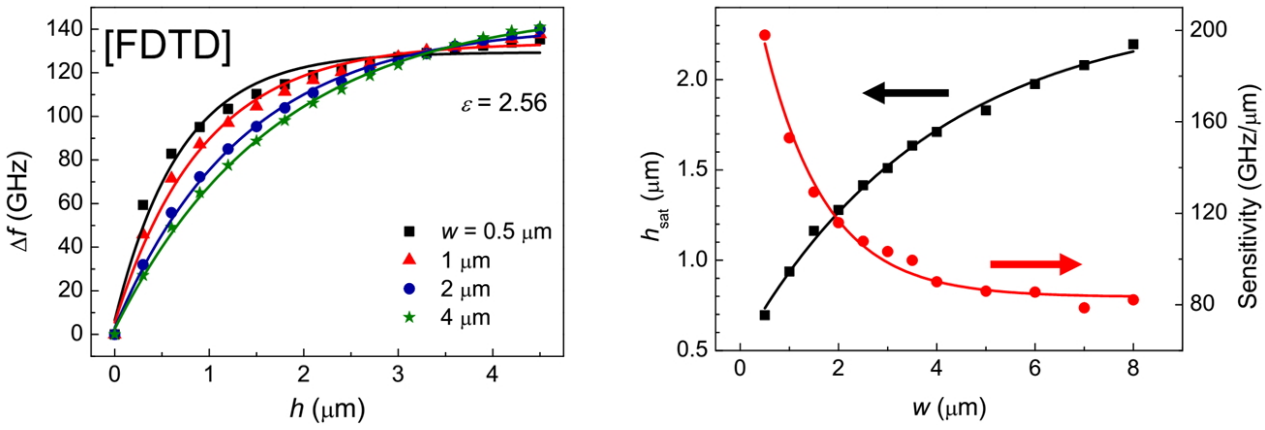

(a) (b)

FIG. 5. (a) FDTD simulation results for Δf as a function of h for various w's in the range 0.5 – 4.0 μm. (b) Saturation thickness (black boxes) and sensitivity (red circles) as a function of w, extracted from FDTD simulations.

and the sensitivity (red circles) as a function of w in the range of 0.5 – 8.0 μm. A clear tendency of decreasing hsat and increasing sensitivity can be observed as w decreases. This is attributable to the relatively large electric field confinement in the case of the small-gap metamaterials. In addition, the simulation results plotted in Fig. 5(b) enabled us to express the saturation thickness quantitatively as a simple exponential decay function of $h_{sat} = 2.4\text{-}1.8\exp(-w/3.9)$. This simple relation offers a very handy tool for estimating the detection volume of metamaterials with various widths, and hence, will be very useful for determining the optimal material thickness to design materials for optimized sensitivity. On the other hand, the sensitivity exhibits different saturation behavior as compared to h_{sat}. This is because sensitivity depends on the total detection volume (not only the vertical range) and is also influenced by various edge effects.

IV. CONCLUSION

In conclusion, we demonstrated the effective detection volume of THz metamaterials as a function of the gap width by quantifying the effective vertical range as a function of the gap width. We measured Δf by spin-coating PMMA layers with various thicknesses onto the metamaterials. The vertical range of the metamaterial detection volume decreased by about 2.5 times as the gap width decreased from 4.0 μm to 0.5 μm. We also performed FDTD simulations, which confirmed our experimental findings and matched our experimental data well. More importantly, we extracted a numerical expression that relates the effective vertical range to the gap width. This information is very useful for many practical applications of THz metamaterials for sensing various dielectric materials both in ambient and aqueous environments. In addition, our work will allow us to understand the essential

operating mechanism of THz metamaterials, and can be extended to studying other various sub-wavelength structures.

ACKNOWLEDGEMENT

This work was supported by Midcareer Researcher Program (2014R1A2A1A11052108) through a National Research Foundation grant funded by the Korea Government (MSIP).

REFERENCES

1. H. T. Chen, W. J. Padilla, R. D. Averitt, A. C. Gossard, C. Highstrete, M. Lee, J. F. O'Hara, and A. J. Taylor, "Electromagnetic metamaterials for terahertz applications," Terahertz Sci. Technol. **1**, 42-50 (2008).
2. S. J. Park, J. T. Hong, S. J. Choi, H. S. Kim, W. K. Park, S. T. Han, J. Y. Park, S. Lee, D. S. Kim, and Y. H. Ahn, "Detection of microorganisms using terahertz metamaterials," Sci. Rep. **4**, 4988 (2014).
3. S. J. Park, S. W. Jun, A. R. Kim, and Y. H. Ahn, "Terahertz metamaterial sensing on polystyrene microbeads: Shape dependence," Opt. Mater. Express **5**, 2150-2155 (2015).
4. S. J. Park, B. H. Son, S. J. Choi, H. S. Kim, and Y. H. Ahn, "Sensitive detection of yeast using terahertz slot antennas," Opt. Express **22**, 30467-30472 (2014).
5. J. B. Pendry, D. Schurig, and D. R. Smith, "Controlling electromagnetic fields," Science **312**, 1780-1782 (2006).
6. R. A. Shelby, D. R. Smith, and S. Schultz, "Experimental verification of a negative index of refraction," Science **292**, 77-79 (2001).
7. H. T. Chen, W. J. Padilla, J. M. O. Zide, A. C. Gossard, A. J. Taylor, and R. D. Averitt, "Active terahertz metamaterial devices," Nature **444**, 597-600 (2006).
8. J. Federici and L. Moeller, "Review of terahertz and subterahertz wireless communications," J. Appl. Phys. **107**, 111101 (2010).
9. R. Marqués, J. Martel, F. Mesa, and F. Medina, "Left-handed-media simulation and transmission of EM waves in subwavelength split-ring-resonator-loaded metallic waveguides," Phys. Rev. Lett. **89**, 183901 (2002).
10. H. O. Moser, B. D. F. Casse, O. Wilhelmi, and B. T. Saw, "Terahertz response of a microfabricated rod-split-ring-resonator electromagnetic metamaterial," Phys. Rev. Lett. **94**, 063901 (2005).
11. J. F. O'Hara, R. Singh, I. Brener, E. Smirnova, J. Han, A. J. Taylor, and W. Zhang, "Thin-film sensing with planar terahertz metamaterials: Sensitivity and limitations," Opt. Express **16**, 1786-1795 (2008).
12. D. J. Park, J. T. Hong, J. K. Park, S. B. Choi, B. H. Son, F. Rotermund, S. Lee, K. J. Ahn, D. S. Kim, and Y. H. Ahn, "Resonant transmission of terahertz waves through metallic slot antennas on various dielectric substrates," Curr. Appl. Phys. **13**, 753-757 (2013).
13. D. J. Park, S. J. Park, I. Park, and Y. H. Ahn, "Dielectric substrate effect on the metamaterial resonances in terahertz frequency range," Curr. Appl. Phys. **14**, 570-574 (2014).
14. S. J. Park and Y. H. Ahn, "Substrate effects on terahertz metamaterial resonances for various metal thicknesses," J. Korean Phys. Soc. **65**, 1843-1847 (2015).
15. J. Li, C. M. Shah, W. Withayachumnankul, B. S.-Y. Ung, A. Mitchell, S. Sriram, M. Bhaskaran, S. Chang, and D. Abbott, "Mechanically tunable terahertz metamaterials," Appl. Phys. Lett. **102**, 121101 (2013).
16. S. J. Park, S. A. N. Yoon, and Y. H. Ahn, "Dielectric constant measurements of thin films and liquids using terahertz metamaterials," RSC Adv. **6**, 69381-69386 (2016).
17. J. T. Hong, D. J. Park, J. H. Yim, J. K. Park, J. Y. Park, S. Lee, and Y. H. Ahn, "Dielectric constant engineering of single-walled carbon nanotube films for metamaterials and plasmonic devices," J. Phys. Chem. Lett. **4**, 3950-3957 (2013).
18. H. R. Park, K. J. Ahn, S. Han, Y. M. Bahk, N. Park, and D. S. Kim, "Colossal absorption of molecules inside single terahertz nanoantennas," Nano Lett. **13**, 1782-1786 (2013).
19. Y. S. Jin, G. J. Kim, and S. G. Jeon, "Terahertz dielectric properties of polymers," J. Korean Phys. Soc. **49**, 513-517 (2006).